633 (1975); M. Hirayama, P. A. Eccleston, D. H. Silberberg, *Dev. Biol.* **104**, 413 (1984)]. Forty-eight hours later, the cells were trypsinized and plated together at a density of 60,000 cells per square centimeter on the wells of duplicate Lab-Tek four-well slides (Nunc Labs) that had been treated with a 1:5 dilution of Vitrogen (Collagen). Twenty-four hours later, fusion medium was added. On the next day, fusion medium supplemented with Ara C was added, and 1 to 2 days later the cells were processed for immunocytochemistry.

10. J. R. Blinks, R. Rudel, S. R. Taylor, *J. Physiol. (London)* **277**, 291 (1977).
11. Enzymatically active β-galactosidase can be detected in both Zc and Zn cells by using X-gal (5-bromo-4-chloro-3-indolyl β-D-galactopyranoside) as substrate. Because *E. coli* β-galactosidase must be at least tetrameric to be active [I. Zabin and A. N. Fowler, in *The Operon*, J. H. Miller and W. S. Reznikoff, Eds. (Cold Spring Harbor Laboratory, Cold Spring Harbor, NY, 1980), pp. 89–121], Zc and Zn fusion proteins probably assemble as tetramers.
12. L. L. Englander and L. L. Rubin, *J. Cell Biol.* **104**, 87 (1987).
13. B. Mintz and W. W. Baker, *Proc. Natl. Acad. Sci. U.S.A.* **58**, 592 (1967); P. M. Frair, P. M. Strasberg, K. B. Freeman, A. C. Peterson, *Biochem. Genet.* **17**, 693 (1979); P. M. Frair and A. C. Peterson, *Exp. Cell Res.* **145**, 167 (1983).
14. If one assumes a diffusion constant (20°C, H_2O) of about 10^{-7} cm^2 s^{-1} for a globular protein of 500,000 kD [C. R. Cantor and P. R. Schimmel, *Biophysical Chemistry, Part II* (Freeman, San Francisco, 1980), p. 584], one can calculate by Einstein's equation, $x^2 = 2\,Dt$ (where x is the distance, D is the diffusion constant, and t is time), that the β-galactosidase fusion protein Zn would diffuse 50 μm in about 2 min. If the effective diffusion constant in cytoplasm is reduced ten-fold (*10*), the corresponding time would be increased to 20 min.
15. C. Bonnerot *et al.*, *Proc. Natl. Acad. Sci. U.S.A.* **84**, 6795 (1987).
16. G. K. Pavlath, K. Rich, S. G. Webster, H. M. Blau, *Nature* **337**, 570 (1989).
17. J. L. Platt and A. F. Michael, *J. Histochem. Cytochem.* **31**, 840 (1983).
18. We thank D. Picard and K. Yamamoto for the plasmids encoding the fusion proteins and for advice and encouragement; N. Fregien for the plasmid ptk-neo; H. Gordon for his help in devising the [^{3}H]thymidine labeling procedure; H. Blau for helpful early discussions; and the members of the laboratory and other colleagues for constructive comments on the manuscript. Supported by grants from NIH (grant NS 20107) and the Muscular Dystrophy Foundation.

15 December 1988; accepted 31 March 1989

Hidden Thermodynamics of Mutant Proteins: A Molecular Dynamics Analysis

JIALI GAO, KRZYSZTOF KUCZERA, BRUCE TIDOR, MARTIN KARPLUS

A molecular dynamics simulation method is used to determine the contributions of individual amino acid residues and solvent molecules to free energy changes in proteins. Its application to the hemoglobin interface mutant Asp G1(99)β→Ala shows that some of the contributions to the difference in the free energy of cooperativity are as large as 60 kilocalories (kcal) per mole. Since the overall free energy change is only −5.5 kcal/mole (versus the experimental value of −3.4 kcal/mole), essential elements of the thermodynamics are hidden in the measured results. By exposing the individual contributions, the free energy simulation provides new insights into the origin of thermodynamic changes in mutant proteins and demonstrates the role of effects beyond those usually considered in structural analyses.

CHANGES IN PROTEIN STABILITY and function resulting from mutations can be determined experimentally. The alterations in free energy are often interpreted in terms of the structures of the wild type and mutant protein (*1, 2*). However, the connection between structure and measured thermodynamic quantities is not simple; for example, relatively small measured free energy changes can be made up of large contributions from a number of protein-protein and protein-solvent interactions that almost cancel. Moreover, the consequences of the removal of repulsive interactions, not usually considered in structural studies, can be as important as the loss of attractive terms (such as hydrogen bonding). We demonstrate how molecular dynamics (MD) free energy simulations can be used to estimate the individual thermodynamic contributions that result from a mutation. The change in the free energy of cooperativity of a mutant of hemoglobin [Asp G1(99)β→Ala] is decomposed into contributions from the solvent, intersubunit interactions, and intrasubunit alterations. The qualitative insights obtained from this decomposition increase our understanding of protein mutants since the effects described for hemoglobin are expected to play a general role.

Department of Chemistry, Harvard University, Cambridge, MA 02138.

The free energy difference ΔG between two states A and B can be calculated by Monte Carlo and MD techniques (*3–7*). If A corresponds to the wild-type protein and B to the mutant, a simulation (which can be envisioned as "computer alchemy" since one amino acid is transformed into another) can be used to determine their free energy difference. The simulation is based on thermodynamic integration (*8*) with the equation

$$\Delta G = G_B - G_A = \int_0^1 \langle \Delta V \rangle_\lambda d\lambda \simeq \sum_i \langle \Delta V \rangle_{\lambda_i} \Delta\lambda \quad (1)$$

where $\Delta V = V_B - V_A$ and λ is a parameter, such that $V_\lambda = (1 - \lambda)V_A + \lambda V_B$ (*9*); V_A and V_B are empirical energy functions describing the solvated normal and mutant hemoglobin molecules, respectively. The calculation uses MD for evaluation of the thermodynamic average, $\langle \Delta V \rangle_\lambda$, where the subscript λ indicates that the average is over the hybrid system described by V_λ. The linear form of Eq. 1 allows the free energy to be decomposed as

$$\Delta G = \Delta G_0 + \sum_{r>0} \Delta G_r \quad (2)$$

where ΔG_0 is the contribution from the free energy change of the mutated residue and ΔG_r ($r > 0$) are the contributions from interactions between the mutated residue and any other residue or water molecule.

The free energy simulation and decomposition method is illustrated for hemoglobin, the classic example of cooperativity (*10–12*). We consider the $\alpha_1\beta_2$ interface residue Asp G1(99)β for which a series of naturally occurring mutants have been shown to have significantly reduced cooperativity and increased oxygen affinity relative to normal hemoglobin (*10, 11, 13*). Based on x-ray structures of deoxy and oxy hemoglobin A, Perutz *et al.* (*14–16*) suggested that the essential role of Asp G1(99)β is to stabilize the deoxy tetramer by making hydrogen bonds to Tyr C7(42)α and to Asn G4(97)α; these hydrogen bonds are absent in the oxy tetramer. We supplement this observational conclusion by a theoretical analysis of the free energy changes induced by the mutation Asp G1(99)β→Ala [Hb Radcliffe (*17*)], which is of the "deletion" type (*1*), and is therefore expected to lead to relatively localized structural changes (*18*) that are simplest to interpret (*19*). The overall change in the free energy of cooperativity (*13*) is shown to result from a set of large but nearly compensating interactions of Asp G1(99)β with several amino acids and with the solvent. Although both Tyr C7(42)α and Asn G4(97)α play a significant role, the calculations indicate that the solvent and other interchain and intrachain interactions are also important.

The essential free energy simulation results are shown in Table 1 (*9, 21, 22*). Energy-minimized unliganded (*23*) and liganded (*24*) x-ray structures for the normal hemoglobin tetramers were used to generate the starting configurations (Fig. 1), and the stochastic boundary molecular dynamics (SBMD) method (*25*) was used for the $\langle \Delta V \rangle_\lambda$ simulations (*26–28*). Both the deoxy and oxy tetramers are destabilized by the mutation (by 66 and 60.5 kcal/mole, respectively, per $\alpha_1\beta_2$ interface) (*29*), but the deoxy tetramer is more destabilized, leading to the observed reduction in cooperativity

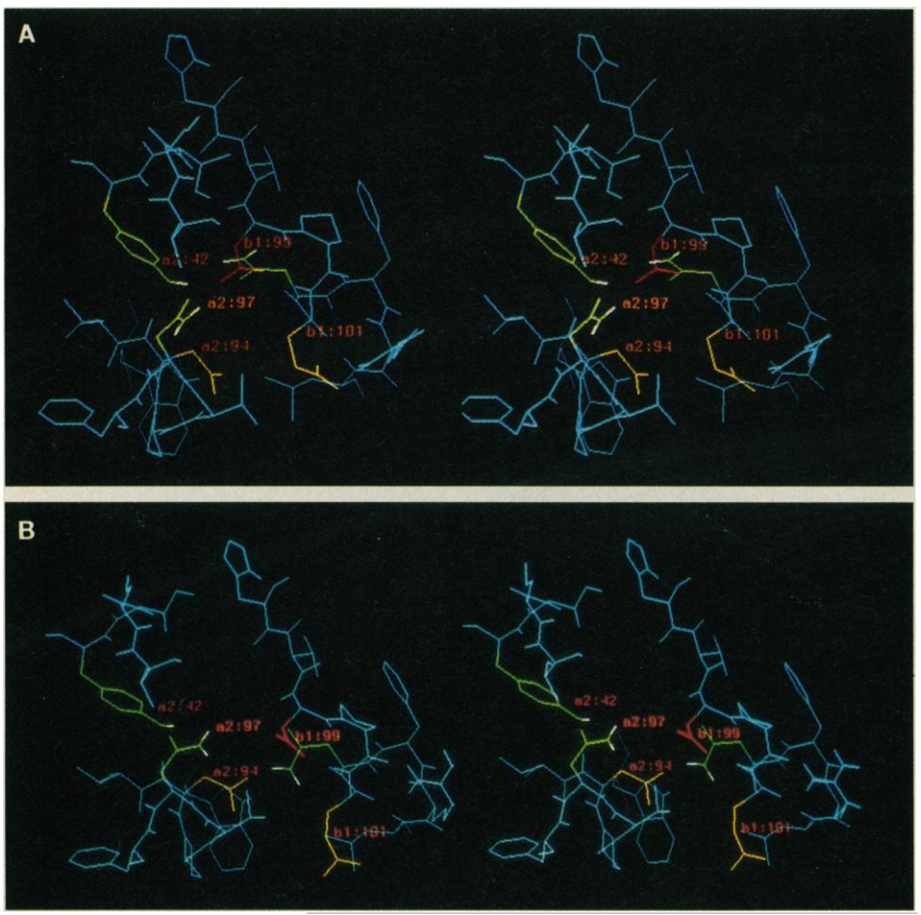

Fig. 1. Stereoviews of the (**A**) deoxy (*23*) and (**B**) oxy (*24*) x-ray structures showing the $\alpha_1\beta_2$ contact region; some of the important side chains are labeled and colored differently from the blue background [Asp G1(99)β is in red]. The deoxy simulation included 87 residues (962 atoms) and 124 water molecules; the oxy simulation included 99 residues (1003 atoms) and 146 water molecules.

Table 1. Free energy (kcal/mole) computed for the mutation Asp G1(99)β → Ala. All values are given for one $\alpha_1\beta_2$ interface; a term in ΔG with a positive sign corresponds to the given contribution destabilizing the mutant (Ala) relative to the wild type (Asp). When the effect of the Asp residue by itself is discussed in the text, a positive sign implies that a stabilizing contribution is involved. ΔΔG is ΔG(oxy) − ΔG(deoxy).

Contribution	ΔG(deoxy)	ΔG(oxy)	ΔΔG
Solvent	46.0	68.5	22.5
Protein*	20.0	−8.0	−28.0
Asp G1(99)β_2†	−8.8	−11.0	−2.2
Inter (α_1)	2.8	−24.4	−27.2
Tyr C7(42)	8.4	4.3	−12.7
Asp G1(94)	−22.0	−44.4	−22.4
Val G3(96)	1.6	7.1	5.5
Asn G4(97)	9.7	13.0	3.3
Intra (β_2)	26.1	27.4	1.3
His FG4(97)	−2.1	−3.3	−1.2
Pro G2(100)	8.2	5.4	−2.8
Glu G3(101)	−11.2	6.9	18.1
Asn G4(102)	14.3	10.1	−4.2
Total	66.0	60.5	−5.5

*Only residues that contribute more than 1.5 kcal/mole to both the deoxy and oxy forms are listed. †Mutant residue self-energy contribution.

and increased affinity of the Ala mutant (*17*). The value of ΔΔG(oxy − deoxy) can be compared with the free energy of cooperativity measured by Ackers and co-workers (*13, 30*). Both the experimental and theoretical thermodynamic cycles (Fig. 2) provide indirect approaches to the change in free energy of cooperativity resulting from the mutation, a quantity that is difficult to obtain directly either experimentally or theoretically. The measured value (−3.4 kcal/mole per interface) has the same sign and is of the same order as the calculated result [−5.5 kcal/mole; other Asp G1(99)β mutants that have been studied experimentally (*13*) yield similar values for ΔΔG], suggesting that the simulation results, although approximate, may be used to obtain insights into the specific interactions that contribute to the free energy differences.

We separated the calculated free energy changes into those arising from the solvent or the protein using Eq. 2; for the latter, we considered the contributions from the same subunit (β_2) and from the different subunit (α_1) and finally decomposed these into individual residue contributions. In most of the following discussion (not in the calculations), we simplify the description by referring to the Asp side chain (see caption to Table 1); the free energy contribution from the mutant (Ala) side chain is small because of its size and nonpolar character.

The structural difference between the deoxy and oxy tetramer x-ray results in the $C\alpha_1$, $FG\beta_2$ region [Asp G1(99)β is adjacent to the FG corner] has been characterized (*14–16, 31, 32*) as an approximately rigid-body displacement, in which $FG\beta_2$ shifts relative to $C\alpha_1$ by approximately 6 Å [the so-called quaternary "switch" (*31*)]. A large alteration in the intersubunit packing occurs with relatively small intrasubunit conformational changes. In the oxy tetramer, the Asp side chain is more exposed to solvent, whereas it is partly buried by interactions with the α subunit in the deoxy tetramer; the difference in accessible surface area for a 1.6 Å probe (*33*) is 13.7 $Å^2$. Thus the large loss in the solvent contribution (Table 1), which is almost entirely due to electrostatic interactions, is more destabilizing for the oxy than the deoxy tetramer. Five water molecules couple strongly to the carboxylate group in the oxy tetramer, whereas only three do so in the deoxy tetramer (Fig. 3). The solvation free energy change calculated for the mutation of the highly exposed Asp in the oxy tetramer (68.5 kcal/mole) is only slightly less than the difference between acetate and ethane in aqueous solution [the experimental value is ~77 kcal/mole (*34*); the value calculated for aqueous solution with the CHARMM 19 charges (*22*) by use of an integral equation method is 75 kcal/mole (*35*)].

The mutation stabilizes the oxy tetramer and destabilizes the deoxy tetramer by an amount that counterbalances the solvent term (Table 1). There are both intersubunit (α_1-β_2) and intrasubunit (β_2-β_2) contributions; the former are more important than the latter. The intersubunit interaction between Asp G1(99)β and Tyr C7(42)α does indeed stabilize the deoxy form in accord with the analysis of Perutz (*10, 14–16*). The total contribution of Tyr C7(42)α, including effects in both the deoxy and the oxy tetramers (Table 1), is somewhat greater than twice the overall calculated free energy difference. All other contributions from interactions with the $C\alpha_1$ region are small. There are, however, large contributions from the G region of the α_1 chain, which is also close to the FG corner of β_2 (Fig. 1). Most important is Asp G1(94)α, which has an unfavorable interaction free energy in both the deoxy and oxy forms [the interaction between Asp G1(94)α and Asp G1(99)β is destabilizing in both tetramers, so that the replacement by the nonpolar Ala stabilizes the system], but the destabilization

is calculated to be much greater in the oxy than the deoxy structure. In the x-ray structures, the two Asp side chains are closer in the oxy than the deoxy tetramer, and the relative orientations are such that the charge-charge repulsions between the oxygens of Asp 94α and Asp 99β are greater in the former than the latter. The simulations show that the unfavorable interactions are balanced by the presence of water-bridged hydrogen bonds between the two Asp carboxylate groups; there are three water bridges in the oxy and two in the deoxy interface. Although macroscopic dielectric treatments (*37, 38*) account, in part, for the balance of protein and solvent interaction, such specific effects are difficult to include in continuum solvent models. In particular, hydrogen bonds involving charged groups lead to highly stable structures because of the strength of the interaction, relative to polar group–water hydrogen bonds (*25*); a carboxylate-water hydrogen bond has an energy of 11 to 15 kcal/mole (*39–41*). For Asn G4(97)α, the simulation shows that the mutation is destabilizing in both structures (Table 1), but that it is somewhat more destabilizing in the oxy than the deoxy form. This result disagrees with suggestions from structural analyses (*10, 14–16*), which focused on an Asp-Asn hydrogen bond that is present in the deoxy and absent in the oxy tetramer. Energy calculations for the x-ray structure show that the Asp G1(99)β–Asn G4(97)α interaction, which is due primarily to the Asp-CO_2^- and Asn-NH_2 moieties, is attractive in both the deoxy and oxy tetramers, as it is in both average dynamics structures; this result is in accord with the destabilizing effect of the mutation obtained from the full simulation. For Val G3(96)α, there is an attractive interaction between the NH of its backbone and the Asp side chain in both structures that is lost when the mutation is introduced.

The contributions that arise from within the β subunit are by definition the result of tertiary structural changes that accompany the quaternary transition. There are the internal energy terms of the Asp and Ala side chains (Table 1) that contribute −2.2 kcal/mole to the free energy difference (*42, 43*). The other residues involved (see Table 1) are all relatively near Asp G1(99)β. The largest contribution arises from Glu G3(101)β. The Asp 99–Glu 101 interaction free energy is calculated to be destabilizing in the deoxy tetramer and stabilizing in the oxy tetramer. The x-ray structures indicate that the side chain of Glu 101 in the deoxy form is closer to Asp G1(99)β (5.70 Å) than in the oxy tetramer (6.10 Å), but that the orientation is such as to minimize the charge repulsion. There is a strong hydrogen bond between the Asp G1(99)β side chain and the main chain NH of Glu G3(101)β that is more favorable in the deoxy than the oxy tetramer [O · · · H distances are 2.1 Å (2.4 Å) for deoxy (oxy)]. The interaction between Asp G1(99)β and Asn G4(102)β is long range, primarily electrostatic in origin, and stabilizing in both tetramers (Table 1). The contributions from His F6(97)β and Pro G2(100)β also arise from electrostatic terms but the difference between the deoxy and oxy tetramers is relatively small.

The analysis has shown how a number of large free energy contributions due to a mutation can yield a small observed change in cooperativity. Such effects are likely to be particularly important when charged side chains are involved. In both the deoxy and oxy tetramers the Asp→Ala mutation leads to an important destabilization (46 and 68.5 kcal/mol, respectively) as a result of the loss of stabilizing interactions with the solvent. This mutation does not produce an unstable protein because the Asp residue presumably is well solvated in the denatured form and a similar (perhaps even larger) destabilization

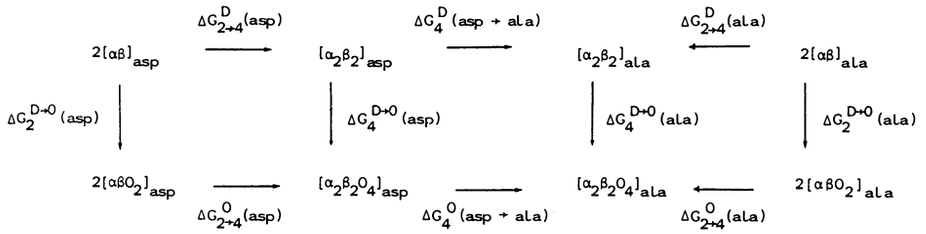

Fig. 2. Diagram showing the thermodynamic cycles used to determine ΔΔG in the calculation (inner cycle) and the experiments (two outer cycles). Superscripts D and O indicate the unliganded and liganded systems, respectively; subscripts 2 and 14 indicate dimers and tetramers, respectively; asp and ala indicate the normal and mutant system, respectively; and the arrow associated with a given ΔG indicates the reaction to which it applies. Horizontal arrows correspond to measured or calculated quantities and vertical arrows to those obtained by difference. The free energy of cooperativity, ΔG_{coop}, is given by $\Delta G_{coop} = \Delta G_4^{D\to O} - \Delta G_2^{D\to O}$ with the assumption that the dimer is noncooperative (*13*). The quantity ΔΔG, the difference in the free energy of cooperativity, is given by $\Delta\Delta G = \Delta G_4^{D\to O}$(ala) − $\Delta G_4^{D\to O}$(asp) if $\Delta G_2^{D\to O}$(asp) = $\Delta G_2^{D\to O}$(ala); it is obtained in the simulation from the inner cycle by calculating ΔG_4^{O}(asp→ala) and ΔG_4^{D}(asp→ala), and it is obtained in the experiment from the outer cycles by measuring [$\Delta G_{2\to4}^{O}$(asp) − $\Delta G_{2\to4}^{D}$(asp)] and [$\Delta G_{2\to4}^{O}$(ala) − $\Delta G_{2\to4}^{D}$(ala)].

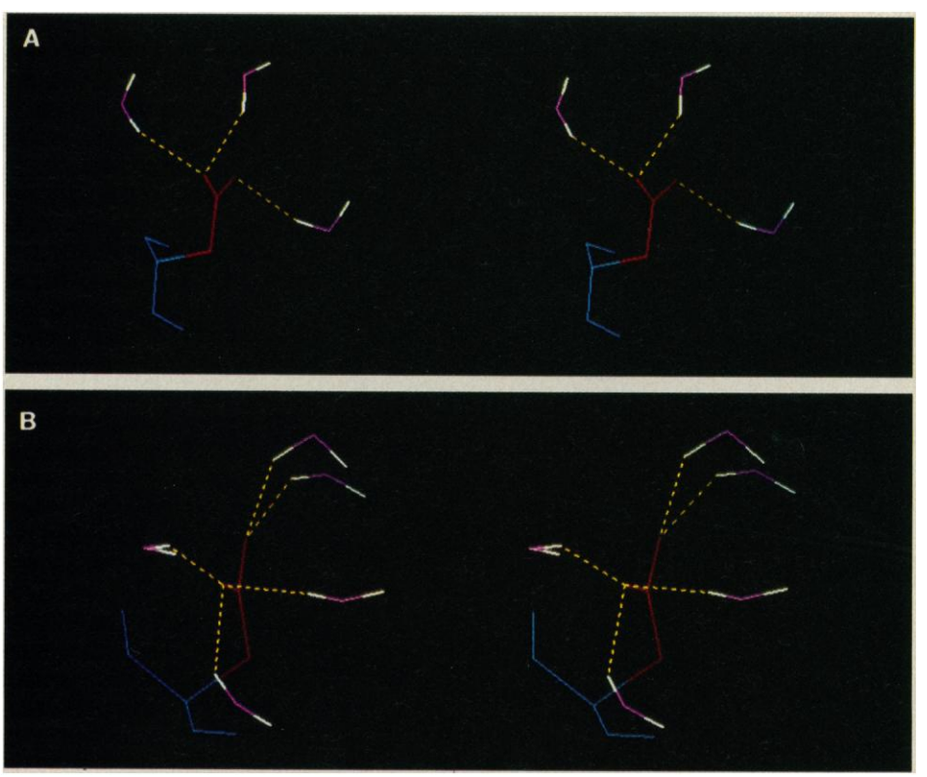

Fig. 3. Stereoviews of water molecules that interact strongly with Asp G1(99)β in the (**A**) deoxy and (**B**) oxy simulations; the minimized average structures are shown. The Asp side chain is in red and the water molecules with the largest interactions are shown as hydrogen bonding to the carboxylate oxygens (waters with distance of 2.3 Å or less are included).

is expected. In contrast, in protein association reactions (insulin dimerization, for example), such a polar to nonpolar mutation can play an important role due to solvation effects; an example is given by sickle cell hemoglobin [Glu A3(6)β→Val], where the mutated residue is exposed in the monomer and partly buried in the dimer (*44*) so that the complex is calculated to be stabilized about 15 kcal/mole per interface (*45, 46*).

REFERENCES AND NOTES

1. A. R. Fersht, *Trends Biochem. Sci.* **12**, 301 (1987).
2. T. Alber *et al.*, *Nature* **330**, 41 (1987).
3. J. P. M. Postma *et al.*, *Faraday Symp.* **17**, 55 (1982).
4. B. L. Tembe and J. A. McCammon, *Comput. Chem.* **8**, 281 (1984).
5. W. L. Jorgensen and C. Ravimohan, *J. Chem. Phys.* **83**, 3050 (1985).
6. P. A. Bash *et al.*, *Science* **235**, 574 (1987).
7. B. M. Pettit and M. Karplus, *Molecular Graphics and Drug Design*, A. S. V. Burgen, G. C. K. Roberts, M. S. Tute, Eds. (Elsevier, New York, 1986), pp. 75–113.
8. J. G. Kirkwood, *J. Chem. Phys.* **3**, 300 (1935); *ibid.* **10**, 394 (1942).
9. S. H. Fleischman *et al.*, unpublished results.
10. R. E. Dickerson and I. Geis, *Hemoglobin: Structure, Function, Evolution, and Pathology* (Benjamin/Cummings, Menlo Park, 1983).
11. H. F. Bunn and B. G. Forget, *Hemoglobin: Molecular, Genetic Clinical Aspects* (Saunders, New York, 1980).
12. M. F. Perutz, G. Fermi, B. Luisi, B. Shaanan, R. C. Liddington, *Acc. Chem. Res.* **20**, 309 (1987).
13. D. W. Pettigrew *et al.*, *Proc. Natl. Acad. Sci. U.S.A.* **79**, 1849 (1982).
14. M. F. Perutz, *Nature* **228**, 726 (1970).
15. ——— and G. Fermi, *Haemoglobin and Myoglobin, Atlas of Molecular Structures in Biology* (New York, Oxford, 1981), vol. 2.
16. M. F. Perutz, *Nature* **232**, 408 (1971).
17. D. J. Weatherall *et al.*, *Brit. J. Haemotology* **35**, 177 (1977).
18. H. H.-L. Shih, J. Brady, M. Karplus, *Proc. Natl. Acad. Sci. U.S.A.* **82**, 1697 (1985).
19. In Hb Yakima [Asp G1(99)β→His], the 3.5 Å resolution difference map for the deoxy tetramer (*20*) indicates that the mutation introduces distributed changes. Although Hb Radcliffe (Asp→Ala) has been examined by x-ray diffraction, a detailed crystallographic study was not made (*17*). However, comparisons of nuclear magnetic resonance (NMR) measurements of unliganded HbA and Hb Radcliffe have been interpreted as showing that it has the deoxy structure in solution, as well as in the crystal, and that there are only "differences in the fine structure between these two hemoglobins."
20. P. D. Pulsinelli, *J. Mol. Biol.* **74**, 57 (1973).
21. All calculations were performed with the CHARMM program (*22*); standard polar hydrogen potential function parameters (CHARMM 19) were used with a unit dielectric constant and the long-range interactions were smoothly truncated to zero at 8.5 Å. The thermodynamic integral is evaluated by the approximation formula given in Eq. 1 with $\langle \Delta V \rangle_\lambda$ determined at a series of values λ_i; in accord with Eq. 1, equally spaced λ_i values (λ_i = 0.1, 0.3, 0.5, 0.7, and 0.9) were used.
22. B. R. Brooks *et al.*, *J. Comp. Chem.* **4**, 187 (1983); the CHARMM 19 charges are CH_2 (−0.16), C (0.36) and O (−0.60) for the Asp side chain and CH_3 (0.0) for the Ala side chain.
23. G. Fermi *et al.*, *J. Mol. Biol.* **175**, 159 (1984).
24. B. Shaanan, *ibid.* **171**, 31 (1983).
25. A. T. Brünger *et al.*, *Proc. Natl. Acad. Sci. U.S.A.* **82**, 8458 (1985). The SBMD method is expected to yield free energies intermediate between the Gibbs and Helmholtz values; for the present mutation, the difference is expected to be small.
26. The molecules were partitioned into MD and Langevin regions with radii of 10 and 15 Å, respectively; the regions were centered on the center-of-mass coordinates of the Asp G1(99)β side chain in the two x-ray structures. The space inside the sphere was filled with water by overlaying a previously equilibrated box of TIP3P water molecules (*27*); the radius for the water sphere was taken to be 14 Å, slightly smaller than the protein sphere, to prevent water molecules from penetrating into the protein core at the boundary region. Water molecules within 2.5 Å of any protein atom were removed from the system. After a 5-ps equilibration of the water structure in the presence of the fixed protein molecule, a second TIP3P overlay was made to fill any voids in the solvent. The calculation of $\langle \Delta V \rangle_\lambda$ for a given λ consisted of a 5-ps equilibration (except for the initial and final integration points, λ = 0.1 and 0.9, where 10-ps equilibrations were used), followed by an averaging period of 5 ps; the coordinates from every fifth time-step were used in the evaluation of $\langle \Delta V \rangle_\lambda$. The simulations were done at 25°C. On a Cray XMP/48, a 5-ps simulation required about 40 min of CPU time with a 1-fs integration step. The variation of $\langle \Delta V \rangle_{\lambda_i}$ with λ_i was monotonic (*28*) and approximately linear. Calculations that used the exponential formula (*4–7*) for ΔG give almost identical values; examination of 1-ps intervals in the 5-ps averages and test studies with smaller λ intervals suggest that the standard deviations of the integrations are ±2 kcal/mole, corresponding to those of other free energy simulations (*4–6*).
27. W. L. Jorgensen *et al.*, *J. Chem. Phys.* **79**, 926 (1983).
28. M. Mezei, *Mol. Phys.* **47**, 1307 (1982).
29. Because the mutation studied does not lead to a balanced reaction, there is some arbitrariness in individual ΔG values. To balance the reaction, the "gas-phase" internal free energy change due to the difference in the number of degrees of freedom in the Asp to Ala mutation (1.4 kcal/mole) can be used.
30. G. K. Ackers, private communication.
31. J. Baldwin and C. Chothia, *J. Mol. Biol.* **129**, 175 (1979).
32. B. R. Gelin *et al.*, *ibid.* **171**, 489 (1983).
33. B. Lee and F. Richards, *J. Biol. Chem.* **55**, 379 (1971).
34. R. G. Pearson, *J. Am. Chem. Soc.* **108**, 6109 (1986); A. Ben-Naim and Y. Marcus, *J. Chem. Phys.* **81**, 2016 (1984).
35. H. Yu and M. Karplus, *J. Chem. Phys.* **89**, 2366 (1988), and unpublished data.
36. M. K. Gilson and B. H. Honig, *Nature* **330**, 84 (1987).
37. D. Bashford, M. Karplus, G. W. Canters, *J. Mol. Biol.* **203**, 507 (1988).
38. In the deoxy x-ray structure (*23*), the Asp-Tyr interaction is repulsive because the two residues are too close together; a constrained minimization leads to a small, relative displacement of the two residues and a stabilizing interaction energy of −14.3 kcal/mole. This value is very close to the calculated value (−13.6 kcal/mole) from the minimized average dynamics structure; the calculated value in the oxy structure is −0.45 kcal/mole.
39. M. Meot-Ner, *J. Am. Chem. Soc.* **110**, 3854 (1988).
40. J. Gao *et al.*, *ibid.* **108**, 4784 (1986).
41. The calculated value with the CHARMM potential (*22*) for the interaction energy between $CH_3CO_2^-$ and a hydrogen-bonding water molecule is −11 to −13 kcal/mole.
42. Neglect of the internal energy contributions to the free energy difference, as was done, for example, in (*6*), yields a calculated ΔΔG value of −3.3 kcal/mole, in even better agreement with the measured value (−3.4 kcal/mole).
43. Although statistical error estimates for free energy simulation can be made, it is not yet possible to determine the systematic errors; see C. L. Brooks III *et al.*, *Proteins: A Theoretical Perspective of Dynamics, Structure and Thermodynamics* (Wiley, New York, 1988).
44. B. C. Wishner, K. B. Ward, E. E. Lattman, W. E. Love, *J. Mol. Biol.* **98**, 179 (1975).
45. K. Kuczera *et al.*, unpublished results.

46. We thank P. A. Bash, D. A. Case, W. Eaton, and S. C. Harrison for comments on the manuscript. The National Institutes of Health, the National Science Foundation, and the Department of Energy provided partial support for this research. The calculations were done mainly on a CRAY X-MP at the Pittsburgh Supercomputer Center and a Convex C1 at Harvard University.

29 November 1988; accepted 3 March 1989

Brefeldin A Specifically Inhibits Presentation of Protein Antigens to Cytotoxic T Lymphocytes

JONATHAN W. YEWDELL AND JACK R. BENNINK

Cytotoxic T lymphocytes (CTLs) recognize foreign antigens, including viral proteins, in association with major histocompatibility complex (MHC) class I molecules. Brefeldin A, a specific inhibitor of exocytosis, completely and reversibly inhibited the presentation of viral proteins, but not exogenous peptides, to MHC class I–restricted CTLs directed against influenza virus antigens. The effect of brefeldin A on antigen presentation correlated with its inhibition of intracellular transport of newly synthesized class I molecules. Brefeldin A is thus a specific inhibitor of antigen processing for class I–restricted T cell recognition. Its effect on antigen presentation supports the idea that exogenous peptide antigens associate with cell surface class I molecules, whereas protein antigens processed via the cytosolic route associate with nascent class I molecules before they leave the trans-Golgi complex.

CYTOTOXIC T LYMPHOCYTES (CTLs) are a critical component of the immune response to infectious agents and neoplasms. Some of the general features of CTL recognition of foreign antigens are understood: (i) epitopes recognized by CTLs are linear determinants that can be replaced by short synthetic peptides (*1*); (ii) nonfragmented proteins must be delivered to the cytosol of target cells to be processed for presentation to CTLs (*2, 3*); and (iii) foreign proteins are recognized by CTLs only in association with class I molecules of the major histocompatibility complex (MHC) (*4*).

Laboratory for Viral Diseases, National Institute of Allergy and Infectious Diseases, Rockville, MD 20852.